



Stoneley wave propagation in transversely isotropic thermoelastic medium with two temperature and rotation

Iqbal Kaur¹ · Parveen Lata¹

Received: 23 July 2019 / Accepted: 6 January 2020 / Published online: 17 January 2020
© Springer-Verlag GmbH Germany, part of Springer Nature 2020

Abstract

In the present paper we studied Stoneley wave propagation at the interface of two dissimilar homogeneous transversely isotropic thermoelastic media with two temperatures and rotation. The secular equations of Stoneley waves are derived in the form of the determinant by using appropriate boundary conditions. The wave characteristics such as phase velocity and attenuation coefficients are computed and depicted graphically. Effect of rotation and two temperature has been depicted on the phase velocity, attenuation coefficient, displacement component, stress component, and Temperature distribution change. Some particular cases are also deduced from the present investigation.

Keywords Transversely isotropic · Thermoelastic · Rotation · Stoneley wave propagation · Two temperature · Energy dissipation

Mathematics Subject Classification 35Lxx · 74Jxx · 74Bxx · 80A20 · 74F05

List of symbols

δ_{ij}	Kronecker delta
C_{ijkl}	Elastic parameters
β_{ij}	Thermal elastic coupling tensor
T	Absolute temperature
T_0	Reference temperature
φ	Conductive temperature
t_{ij}	Stress tensors
e_{ij}	Strain tensors
u_i	Components of displacement
ρ	Medium density

✉ Iqbal Kaur
bawahanda@gmail.com

Parveen Lata
parveenlata@pbi.ac.in

¹ Department of Basic and Applied Sciences, Punjabi University, Patiala, Punjab, India

C_E	Specific heat
α_{ij}	Linear thermal expansion coefficient
K_{ij}^*	Thermal conductivity
ω	Angular frequency
Ω	Angular velocity of the solid and equal to $\Omega \mathbf{n}$, where \mathbf{n} is a unit vector
\vec{u}	Displacement vector
F_i	Components of Lorentz force
τ_0	Relaxation time
ε_0	Electric permeability
$\delta(t)$	Dirac's delta function
ξ	Wavenumber
C_1	Longitudinal wave velocity
a_{ij}	Two temperature parameters

1 Introduction

A Stoneley wave is an interface wave that usually travels along with the interface of two solids. Moreover, when initiates at the interface of liquid and solid, this wave is known as Scholte wave. This wave has maximum intensity at the boundary and decreases exponentially away from it. The wave generated by the sonic tool in a bore well is the example of these types of waves. Stoneley wave's analysis provides information about the positions of fractures and permeability of the formation. These waves not only deliver better information about the internal structure of the earth but are also helpful in the assessment of valuable materials under the earth's surface. Stoneley waves are a major source of noise in vertical seismic profiles. These waves help in the study of geophysics, seismological processes, ocean acoustics, SAW devices, and non-destructive evaluation.

Stoneley (1924) firstly studied the existence of these waves propagating at the interface of two solid, solid–liquid medium and derived the Stoneley wave's dispersion equation. Tajuddin (1995) studied the presence of Stoneley waves at the boundary of two micropolar elastic half-spaces. Ting (2004) explored a surface wave propagation in an anisotropic rotating medium. Othman and Song (2006, 2008) presented different hypotheses about magneto-thermo-elastic waves in a homogeneous and isotropic medium. Abo-Dahab (2013, 2015) studied the different forms of surface waves. Kumar et al. (2013) investigated the Stoneley waves propagation at the boundary of two couple stress thermoelastic medium with LS and GL theories. Mahmoud (2014) studied the effect of the magnetic field, gravity field, and rotation on the propagation of Rayleigh waves in an initially stressed non-homogeneous orthotropic medium. Lata et al. (2016) investigated plane waves in an anisotropic thermoelastic. Abd-Alla et al. (2017) explored the propagation of surface waves in fiber-reinforced anisotropic media of n th order with rotation and magnetic field. Singh and Tochwang (2019) studied the propagation of surface waves at the bonded and unbonded interfaces with voids. Despite of this numerous investigators worked on diverse thermoelasticity theories as Marin (1999), Marin et al. (2016), Kumar et al. (2016), Marin and Craciun

(2017), Ezzat et al. (2017), Hassan et al. (2018), Othman and Marin (2017), Lata and Kaur (2019a, b, c) and Lata and Kaur (2019d, e).

In this paper, we have studied the Stoneley wave propagation at the interface of two dissimilar transversely isotropic thermoelastic homogeneous media with two temperature and rotation. Keeping in view of this, dispersion equation for Stoneley waves at the interface of two different TIT mediums with two temperature and rotation have been derived. Numerical methods are used to study the variation of displacement component, stress component, Temperature, phase velocity, and attenuation coefficient w.r.t. wave number.

2 Basic equations

The basic governing equations for homogeneous, anisotropic, generalized thermoelastic solids in the absence of body forces, heat sources following Chandrasekharaiah (1998), Youssef (2011) and Green and Naghdi (1992) are

$$t_{ij} = C_{ijkl}e_{kl} - \beta_{ij}T, \tag{1}$$

$$K_{ij}^*\varphi_{ij} = \beta_{ij}T_0\ddot{e}_{ij} + \rho C_E\ddot{T} \tag{2}$$

where

$$\beta_{ij} = C_{ijkl}\alpha_{ij},$$

$$e_{ij} = \frac{1}{2}(u_{i,j} + u_{j,i}), \quad i, j = 1, 2, 3.$$

$$T = \varphi - a_{ij}\varphi_{,ij},$$

$$\beta_{ij} = \beta_i\delta_{ij}, \quad K_{ij}^* = K_i^*\delta_{ij} \quad i \text{ is not summed.}$$

Here, c_{ijkl} ($c_{ijkl} = c_{klij} = c_{jikl} = c_{ijlk}$) are elastic parameters and having symmetries due to

1. The stress tensor is symmetric, which is only possible if ($C_{ijkl} = C_{jikl}$)
2. If a strain energy density exists for the material, the elastic stiffness tensor must satisfy $C_{ijkl} = C_{klij}$
3. From stress tensor and elastic stiffness tensor symmetries infer ($C_{ijkl} = C_{ijlk}$) and $C_{ijkl} = C_{klij} = C_{jikl} = C_{ijlk}$

Equation of motion as described by Schoenberg and Censor (1973) for an homogeneous transversely isotropic (HTI) medium rotating uniformly with an angular velocity Ω

$$t_{ij,j} = \rho\{\ddot{u}_i + (\Omega \times (\Omega \times u))_i + (2\Omega \times \dot{u}_i)\}, \tag{3}$$

The terms $\Omega \times (\Omega \times u)$ and $2\Omega \times \dot{u}$ are the centripetal acceleration and Coriolis acceleration due to the time-varying motion respectively.

3 Formulation of the problem

We consider a perfectly conducting homogeneous TIT half-space M_1 with rotation overlying another homogeneous, transversely isotropic thermoelastic half-space M_2 with rotation connecting at the interface $z = 0$. We take the origin of the coordinate system (x, y, z) on $(z = 0)$. We choose x-axis in the direction of wave propagation in such a way that all the particles on a line parallel to the y-axis are equally displaced, so that $v = 0$ and u, w, φ are independent of y . Medium M_2 occupies the region $-\infty < z \leq 0$ and the medium M_1 occupies the region $0 \leq z < \infty$. The plane signifies the boundary among the two medium M_1 and M_2 . The quantities represented for the medium M_1 are without bar and with bar for medium M_2 . For the 2D problem in xz -plane, we take (Fig. 1)

$$u = (u, 0, w).$$

Now using the transformation on Eqs. (1)–(2) following Slaughter (2002) is as under:

$$\begin{aligned}
 & C_{11} \frac{\partial^2 u}{\partial x^2} + C_{13} \frac{\partial^2 w}{\partial x \partial z} + C_{44} \left(\frac{\partial^2 u}{\partial z^2} + \frac{\partial^2 w}{\partial x \partial z} \right) - \beta_1 \frac{\partial}{\partial x} \left\{ \varphi - \left(a_1 \frac{\partial^2 \varphi}{\partial x^2} + a_3 \frac{\partial^2 \varphi}{\partial z^2} \right) \right\} \\
 & = \rho \left(\frac{\partial^2 u}{\partial t^2} - \Omega^2 u + 2\Omega \frac{\partial w}{\partial t} \right), \tag{4}
 \end{aligned}$$

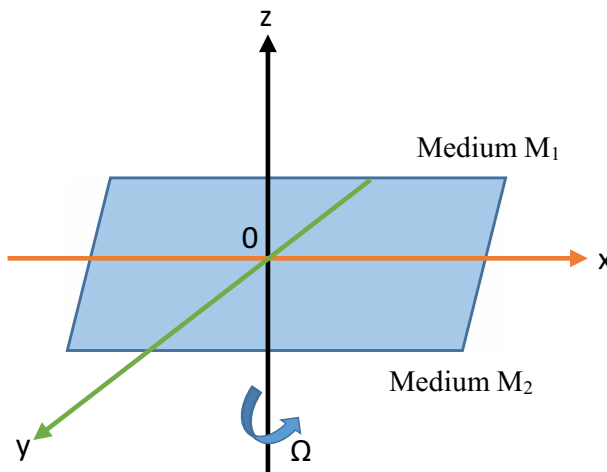


Fig. 1 Geometry of the problem

$$\begin{aligned} & (C_{13} + C_{44}) \frac{\partial^2 u}{\partial x \partial z} + C_{44} \frac{\partial^2 w}{\partial x^2} + C_{33} \frac{\partial^2 w}{\partial z^2} - \beta_3 \frac{\partial}{\partial z} \left\{ \varphi - \left(a_1 \frac{\partial^2 \varphi}{\partial x^2} + a_3 \frac{\partial^2 \varphi}{\partial z^2} \right) \right\} \\ & = \rho \left(\frac{\partial^2 w}{\partial t^2} - \Omega^2 w - 2\Omega \frac{\partial u}{\partial t} \right), \end{aligned} \tag{5}$$

$$K_1^* \frac{\partial^2 \varphi}{\partial x^2} + K_3^* \frac{\partial^2 \varphi}{\partial z^2} = \left[\rho C_E \frac{\partial^2}{\partial t^2} \left\{ \varphi - \left(a_1 \frac{\partial^2 \varphi}{\partial x^2} + a_3 \frac{\partial^2 \varphi}{\partial z^2} \right) \right\} + T_0 \left\{ \beta_1 \frac{\partial \ddot{u}}{\partial x} + \beta_3 \frac{\partial \ddot{w}}{\partial z} \right\} \right]. \tag{6}$$

and

$$t_{xx} = C_{11}e_{xx} + C_{13}e_{xz} - \beta_1 T, \tag{7}$$

$$t_{zz} = C_{13}e_{xx} + C_{33}e_{zz} - \beta_3 T, \tag{8}$$

$$t_{xz} = 2C_{44}e_{xz}, \tag{9}$$

where

$$\beta_1 = (C_{11} + C_{12})\alpha_1 + C_{13}\alpha_3, \tag{10}$$

$$\beta_3 = 2C_{13}\alpha_1 + C_{33}\alpha_3, \tag{11}$$

Using dimensionless quantities:

$$\begin{aligned} (x', z') &= \frac{1}{L}(x, z), (u', w') = \frac{\rho C_1^2}{L\beta_1 T_0}(u, w), \rho C_1^2 = C_{11}, (T', \varphi') = \frac{1}{T_0}(T, \varphi), \\ t' &= \frac{C_1}{L}t, (t'_{xx}, t'_{xz}, t'_{zz}) = \frac{1}{\beta_1 T_0}(t_{xx}, t_{xz}, t_{zz}), (a'_1, a'_3) = \frac{1}{L^2}(a_1, a_3), \Omega' = \frac{L}{C_1}\Omega. \end{aligned} \tag{12}$$

With the use of (12) in Eqs. (4)–(6), and suppressing the primes, we get

$$\frac{\partial^2 u}{\partial x^2} + \delta_2 \frac{\partial^2 w}{\partial x \partial z} + \delta_1 \frac{\partial^2 u}{\partial z^2} - \frac{\partial}{\partial x} \left\{ \varphi - \left(a_1 \frac{\partial^2 \varphi}{\partial x^2} + a_3 \frac{\partial^2 \varphi}{\partial z^2} \right) \right\} = \left(\frac{\partial^2 u}{\partial t^2} - \Omega^2 u + 2\Omega \frac{\partial w}{\partial t} \right), \tag{13}$$

$$\delta_2 \frac{\partial^2 u}{\partial x \partial z} + \delta_1 \frac{\partial^2 w}{\partial x^2} + \delta_3 \frac{\partial^2 w}{\partial z^2} - \delta_5 \frac{\partial}{\partial z} \left\{ \varphi - \left(a_1 \frac{\partial^2 \varphi}{\partial x^2} + a_3 \frac{\partial^2 \varphi}{\partial z^2} \right) \right\} = \left(\frac{\partial^2 w}{\partial t^2} - \Omega^2 w - 2\Omega \frac{\partial u}{\partial t} \right), \tag{14}$$

$$\left(\frac{\partial^2 \varphi}{\partial x^2} + \delta_6 \frac{\partial^2 \varphi}{\partial z^2} \right) = \left[\delta_8 \frac{\partial^2}{\partial t^2} \left\{ \varphi - \left(a_1 \frac{\partial^2 \varphi}{\partial x^2} + a_3 \frac{\partial^2 \varphi}{\partial z^2} \right) \right\} + \delta_7 \left\{ \frac{\partial u}{\partial x} + \delta_5 \frac{\partial w}{\partial z} \right\} + \right], \tag{15}$$

where

$$\delta_1 = \frac{c_{44}}{c_{11}}, \quad \delta_2 = \frac{c_{13} + c_{44}}{c_{11}}, \quad \delta_3 = \frac{c_{33}}{c_{11}}, \quad \delta_5 = \frac{\beta_3}{\beta_1}, \quad \delta_6 = \frac{K_3^*}{K_1^*}, \quad \delta_7 = \frac{T_0 \beta_1^2}{K_1^* \rho}, \quad \delta_8 = \frac{C_E C_{11}}{K_1^*}.$$

We consider the solution of the form

$$(u, w, \varphi) = (u^*, w^*, \varphi^*)(z)e^{i\xi(x-ct)}, \tag{16}$$

where $c = \omega/\xi$ is the dimensionless phase velocity.

Upon using Eq. (16) in Eqs. (13)–(15) we get

$$u^* [l_1 + \delta_2 D^2] + w^* [l_2 + l_3 D] + \varphi^* [l_4 + l_5 D^2] = 0, \tag{17}$$

$$u^* [-l_2 + l_3 D] + w^* [l_6 + \delta_3 D^2] + \varphi^* [l_7 D + l_8 D^3] = 0, \tag{18}$$

$$u^* [l_9] + w^* [l_{10} D] + \varphi^* [l_{11} + l_{12} D^2] = 0, \tag{19}$$

where

$$l_1 = \xi^2(c^2 - 1), \quad l_2 = 2i\xi c, \quad l_3 = \delta_2 i\xi, \quad l_4 = -i\xi(1 + a_1 \xi^2), \quad l_5 = a_3 i\xi, \\ l_6 = (c^2 - \delta_1)\xi^2 + 1, \quad l_7 = -\delta_5(1 + a_1 \xi^2), \quad l_8 = \delta_5 a_3, \quad l_9 = \delta_7 i\xi^3 c^2, \quad l_{10} = \delta_7 \delta_5 \xi^2 c^2, \\ l_{11} = \delta_8 \xi^2 c^2(1 + a_1 \xi^2) - \xi^2, \quad l_{12} = -\delta_8 \xi^2 c^2 a_3 + \delta_6.$$

and characteristic equation is a biquadratic equation in D^2 given by

$$D^6 + \frac{B}{A}D^4 + \frac{C}{A}D^2 + \frac{E}{A} = 0, \tag{20}$$

where

$$A = \delta_2 \delta_3 l_{12} - l_{10} \delta_2 l_8,$$

$$B = \delta_3 \delta_2 l_{11} + \delta_2 l_6 l_{12} + l_1 \delta_3 l_{12} - \delta_2 l_{10} l_7 - l_1 l_{10} l_8 - l_1^2 l_{12} + l_8 l_9 l_3 + l_3 l_5 l_{10} - l_5 \delta_3 l_9,$$

$$C = \delta_2 l_{11} l_6 + l_{11} \delta_3 l_1 + l_1 l_6 l_{12} - l_1 l_{10} l_7 + l_1^2 l_{11} + l_2^2 l_{12} - l_3^2 l_{11} + l_3 l_9 l_7 + l_3 l_4 l_{10} - l_5 l_9 l_6 - l_4 \delta_3 l_9,$$

$$E = l_{11} l_1 l_6 - l_9 l_4 l_6,$$

For medium $M_1(z > 0)$

$$(u, w, \varphi) = \sum_{j=1}^3 A_j(1, d_j, k_j) e^{-m_j z} e^{i\xi(x-ct)}, \tag{21}$$

Thus from Eq. (16) and (21)

$$u^* = \sum_{j=1}^3 A_j e^{-m_j z},$$

$$w^* = \sum_{j=1}^3 d_j A_j e^{-m_j z},$$

$$\varphi^* = \sum_{j=1}^3 k_j A_j e^{-m_j z},$$

where

$$d_j = \frac{l_1 l_{11} - l_9 l_4 + (l_{11} \delta_2 + l_1 l_{12} - l_9 l_5) m_j^2 + (\delta_2 l_{12}) m_j^4}{l_6 l_{11} + (l_{11} \delta_3 + l_6 l_{12} - l_{10} l_7) m_j^2 + (\delta_3 l_{12} - l_{10} l_8) m_j^4}, \tag{22}$$

$$k_j = \frac{l_1 l_6 + l_2^2 + (l_6 \delta_2 + l_1 \delta_3 - l_2^2) m_j^2 + (\delta_2 \delta_3) m_j^4}{l_6 l_{11} + (l_{11} \delta_3 + l_6 l_{12} - l_{10} l_7) m_j^2 + (\delta_3 l_{12} - l_{10} l_8) m_j^4}. \tag{23}$$

For medium M_2 ($z > 0$) we will attach a bar

$$(\bar{u}, \bar{w}, \bar{\varphi}) = (1, \bar{d}_j, \bar{k}_j) e^{\bar{m}_j z} \bar{A}_j e^{i\bar{\xi}(x-ct)},$$

where quantities $\bar{u}, \bar{w}, \bar{\varphi}, \bar{d}_j, \bar{k}_j, \bar{A}_j, \bar{m}_j$ are obtained by attaching bars in the above expressions.

4 Boundary conditions

We consider that both half-spaces are in perfect contact. Thus, there is the stability of components of the displacement vector, stress vector, and temperature change at the interface.

The boundary conditions at $z=0$ are given by

$$t_{zz} = \bar{t}_{zz}, \quad t_{zx} = \bar{t}_{zx}, \quad \varphi = \bar{\varphi}, \quad u = \bar{u}, \quad w = \bar{w}, \quad K_3^* \frac{\partial \varphi}{\partial z} = \bar{K}_3^* \frac{\partial \bar{\varphi}}{\partial z}. \tag{24}$$

5 Derivations of the secular equations

By using the values of $u, w, \varphi, \bar{u}, \bar{w}, \bar{\varphi}$ in (24), we get six linear equations as:

$$\sum_{j=1}^3 Q_{pj} A_j + \sum_{j=1}^3 Q_{p(j+3)} \bar{A}_j = 0, p = 1, 2, 3, 4, 5, 6.$$

where

$$Q_{1j} = i\xi - \delta_9 d_j m_j - (1 + a_1 \xi^2 - a_3 m_j^2) k_j, Q_{1(j+3)} = -i\xi - \delta_9 \bar{d}_j \bar{m}_j + (1 + a_1 \xi^2 - a_3 \bar{m}_j^2) \bar{k}_j,$$

$$Q_{2j} = -m_j + d_j i\xi, Q_{2(j+3)} = -m_j - d_j i\xi,$$

$$Q_{3j} = k_j, Q_{3(j+3)} = -\bar{k}_j,$$

$$Q_{4j} = \delta_1 m_j^2 + (2i\xi c - \delta_2 i\xi m_j) d_j + (-i\xi(1 + a_1 \xi^2) + a_3 i\xi m_j^2) k_j,$$

$$Q_{4(j+3)} = -\delta_1 \bar{m}_j^2 - (2i\xi c - \delta_2 i\xi \bar{m}_j) \bar{d}_j - (-i\xi(1 + a_1 \xi^2) + a_3 i\xi \bar{m}_j^2) \bar{k}_j,$$

$$Q_{5j} = -2\delta_4 i\xi c - \delta_2 i\xi m_j + \delta_3 m_j^2 d_j - \delta_5 (-(1 + a_1 \xi^2) m_j + a_3 m_j^3) k_j,$$

$$Q_{5(j+3)} = 2\delta_4 i\xi c - \delta_2 i\xi \bar{m}_j + \delta_3 \bar{m}_j^2 \bar{d}_j + \delta_5 (-(1 + a_1 \xi^2) \bar{m}_j + a_3 \bar{m}_j^3) \bar{k}_j,$$

$$Q_{6j} = -K_3^* \bar{k}_j \bar{m}_j. \tag{25}$$

The system of Eqs. (25) has a non-trivial solution if the determinant of unknowns $A_j, \bar{A}_j, j = 1, 2, 3$ vanishes i.e.

$$|Q_{ij}|_{6 \times 6} = 0.$$

These secular equations have entire information regarding the wavenumber, phase velocity, and attenuation coefficient of Stoneley waves in the TIT medium.

6 Particular cases

If $C_{11} = C_{33} = \lambda + 2\mu, C_{12} = C_{13} = \lambda, C_{44} = \mu, \alpha_1 = \alpha_3 = \alpha', \beta_1 = \beta_3 = \beta, K_1^* = K_3^* = K^*$ we obtain expressions for Stoneley wave propagation in isotropic materials with rotation.

7 Numerical results and discussion

To demonstrate the theoretical results and effect of rotation and two temperatures, we now present some numerical results. Following Kumar et al. (2017), copper material has been taken for TIT material as medium 1,

Quantity	Value	Unit
c_{11}	18.78×10^{10}	$\text{Kg m}^{-1} \text{s}^{-2}$
c_{12}	8.76×10^{10}	$\text{Kg m}^{-1} \text{s}^{-2}$
c_{33}	17.2×10^{10}	$\text{Kg m}^{-1} \text{s}^{-2}$
c_{13}	8.0×10^{10}	$\text{Kg m}^{-1} \text{s}^{-2}$
c_{44}	5.06×10^{10}	$\text{Kg m}^{-1} \text{s}^{-2}$
β_1	7.543×10^6	$\text{N m}^{-2} \text{deg}^{-1}$
β_3	9.208×10^6	$\text{N m}^{-2} \text{deg}^{-1}$
ρ	8.954×10^3	kg m^{-3}
C_E	4.27×10^2	$\text{JKg}^{-1} \text{deg}^{-1}$
K_1^*	0.04×10^2	$\text{N s}^{-2} \text{deg}^{-1}$
K_3^*	0.02×10^2	$\text{N s}^{-2} \text{deg}^{-1}$
T_0	293	deg
α_1	2.98×10^{-5}	K^{-1}
α_3	2.4×10^{-5}	K^{-1}

Following Kumar et al. (2017), magnesium material has been taken for thermoelastic material as medium 2:

Quantity	Value	Unit
\bar{c}_{11}	5.974×10^{10}	$\text{Kg m}^{-1} \text{s}^{-2}$
\bar{c}_{12}	2.624×10^{10}	$\text{Kg m}^{-1} \text{s}^{-2}$
\bar{c}_{33}	6.17×10^{10}	$\text{Kg m}^{-1} \text{s}^{-2}$
\bar{c}_{13}	2.17×10^{10}	$\text{Kg m}^{-1} \text{s}^{-2}$
\bar{c}_{44}	3.278×10^{10}	$\text{Kg m}^{-1} \text{s}^{-2}$
$\bar{\beta}_1$	2.68×10^6	$\text{N m}^{-2} \text{deg}^{-1}$
$\bar{\beta}_3$	2.68×10^6	$\text{N m}^{-2} \text{deg}^{-1}$
$\bar{\rho}$	1.74×10^3	kg m^{-3}
\bar{C}_E	1.04×10^3	$\text{JKg}^{-1} \text{deg}^{-1}$
\bar{K}_1^*	0.02×10^2	$\text{N s}^{-2} \text{deg}^{-1}$
\bar{K}_3^*	0.02×10^2	$\text{N s}^{-2} \text{deg}^{-1}$
\bar{T}_0	293	deg
$\bar{\alpha}_1$	2.98×10^{-5}	K^{-1}
$\bar{\alpha}_3$	2.4×10^{-5}	K^{-1}

Using the above values, the graphical representations of stress components, temperature change, wave velocity, attenuation coefficient depth of Stoneley wave

in TIT medium have been investigated with two temperature and rotation and demonstrated graphically as:

Case-I: Effect of rotation

1. The solid line relates to $\Omega = 0$,
2. The dashed line relates to $\Omega = 0.5$,
3. The dotted line relates to $\Omega = 1.0$.

Figure 2 demonstrates the Stoneley wave's attenuation coefficient w.r.t. ξ for different values of rotation. It is clear from the graph, as we increase the rotation, the attenuation coefficient is declined. Near the interface of the two material, the attenuation coefficient is very high and below the boundary surface, it declines to zero for all the cases of rotation. Figure 3 shows the Stoneley wave's phase velocity w.r.t. ξ for different values of rotation. It is clear from the graph, as we increase the rotation, the phase velocity is increased. Near the interface of the two material, the phase velocity is very high when $\Omega = 1.0$ and below the boundary surface, it comes to steady-state. Moreover, near the interface of the two material, the phase velocity is increased when $\Omega = 0.0$ and 0.5 and below boundary surface it comes to steady-state for both the cases of rotation.

Figure 4 shows the magnitude values of Temperature distribution w.r.t. ξ for different values of rotation. It is clear from the graph, as we increase the rotation, the magnitude values of the Temperature Distribution of the Stoneley wave is increased. Near the interface of the two material, the magnitude values of the temperature of the Stoneley wave are very high when $\Omega = 1.0$ and below the boundary surface, it comes to steady-state. Moreover, near the interface of the two material the magnitude values of the temperature of Stoneley wave show the opposite behavior when

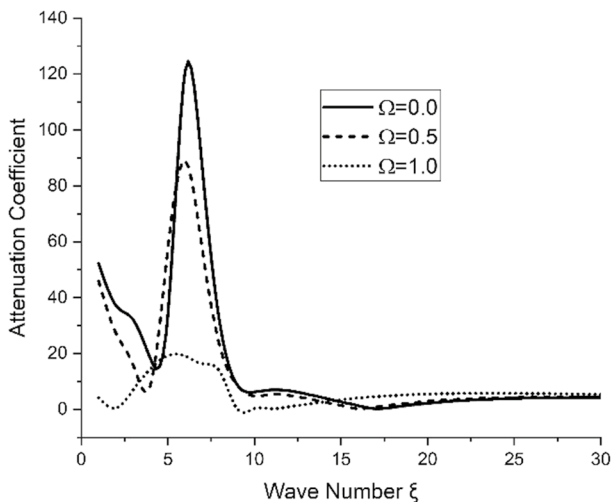


Fig. 2 Variation of Stoneley waves attenuation coefficient w.r.t. ξ

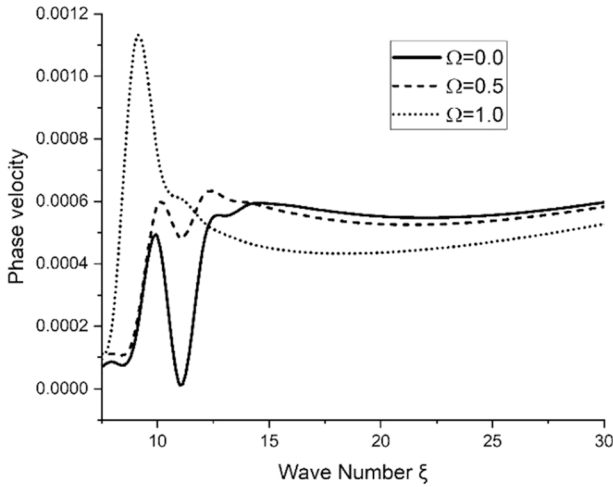


Fig. 3 Variation of Stoneley waves velocity w.r.t. ξ

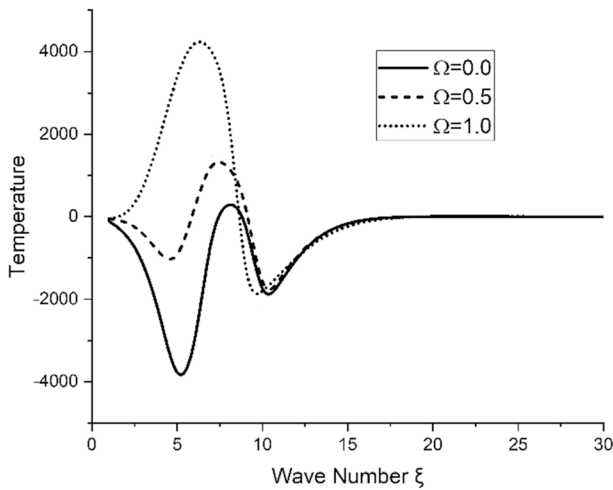


Fig. 4 Variation of Temperature distribution w.r.t. ξ

$\Omega = 0.0$ and 0.5 and below boundary surface it comes to steady-state for both the cases of rotation. Figure 5 demonstrates the Stoneley wave's displacement component w w.r.t. ξ for different values of rotation. It is clear from the graph, as we increase the rotation, the displacement component w of Stoneley wave declines. Near the interface of the two material the displacement component w of Stoneley wave is very high and below boundary surface, it declines to zero for all the cases of rotation.

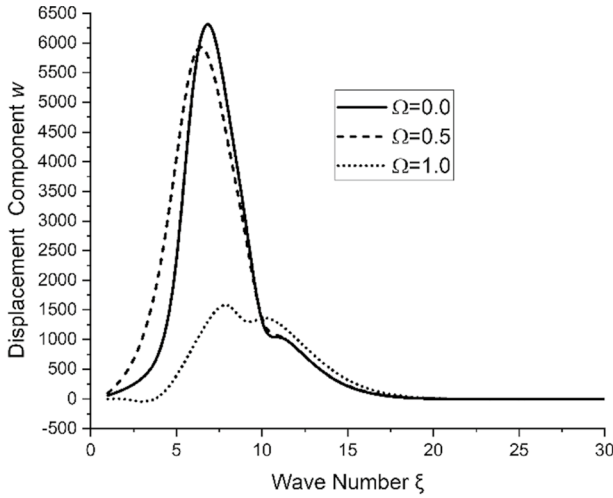


Fig. 5 Variation of Stoneley waves displacement component w w.r.t. ξ

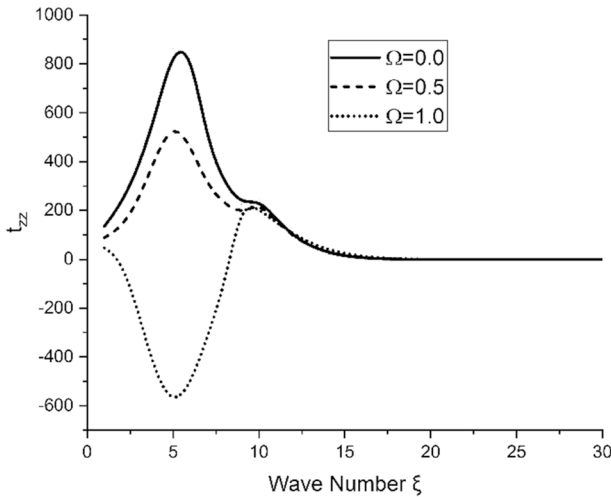


Fig. 6 Variation of Stoneley waves stress component T_{zz} w.r.t. ξ

Figure 6 illustrates the stress component t_{zz} w.r.t. ξ for different values of rotation. It is clear from the graph, as we increase the rotation, the stress component t_{zz} of the Stoneley wave is varied. Near the interface of the two material, the t_{zz} of Stoneley wave is very high when $\Omega = 1.0$ and below boundary surface, it comes to steady-state. Moreover, near the interface of the two material, the t_{zz} of Stoneley wave shows the opposite behavior when $\Omega = 0.0$ and 0.5 and below boundary surface it comes to steady-state for both the cases of rotation.

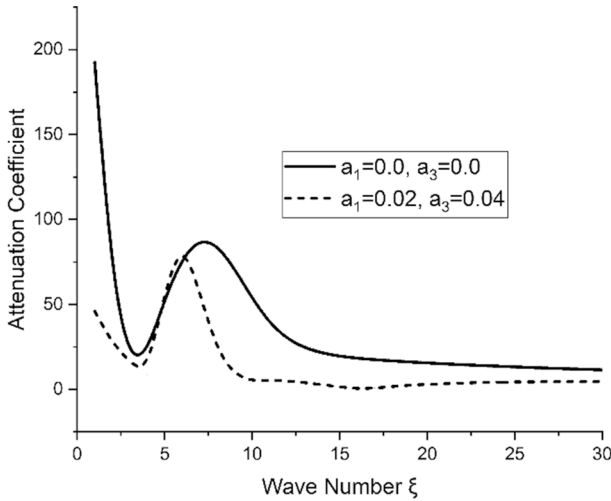


Fig. 7 Variation of Stoneley waves attenuation coefficient w.r.t. ξ

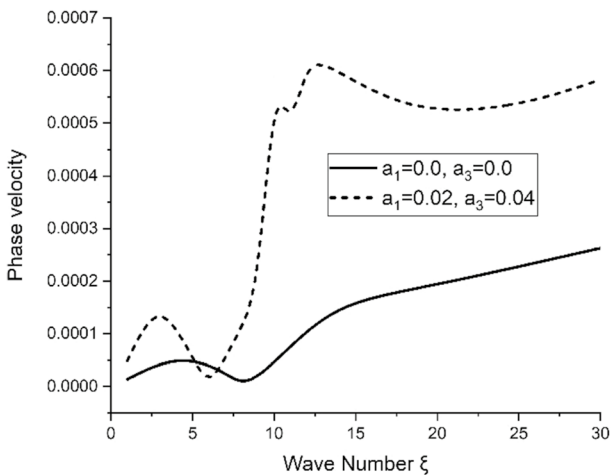


Fig. 8 Variation of Stoneley waves velocity w.r.t. ξ

Case-II: Effect of two temperature

1. The solid line relates to $a_1 = a_3 = 0$,
2. The dashed line relates to $a_1 = 0.2, a_3 = 0.4$.

Figure 7 demonstrates the Stoneley wave’s attenuation coefficient w.r.t. ξ with and without two temperatures. It is clear from the graph, with two temperatures, the attenuation coefficient is declined. Near the interface of the two material, the attenuation coefficient is very high and below the boundary surface, it declines to zero

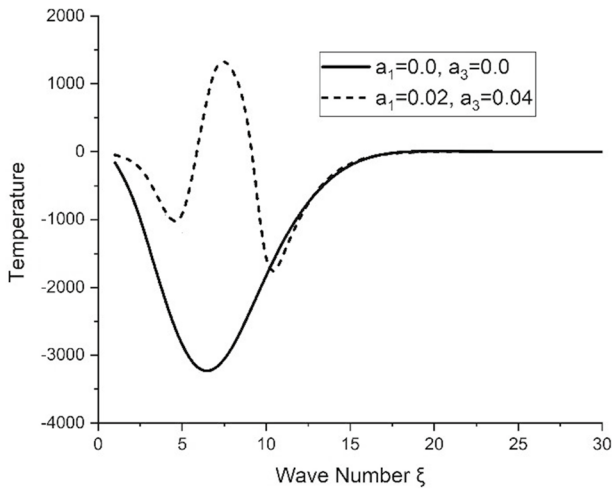


Fig. 9 Variation of temperature distribution T w.r.t. ξ

in absence and presence of two temperatures. Figure 8 shows the Stoneley wave's phase velocity w.r.t. ξ with and without two temperatures. It is clear from the graph, with two temperatures, the phase velocity of the Stoneley wave is increased.

Figure 9 shows the magnitude values of Temperature distribution w.r.t. ξ with and without two temperatures. It is clear from the graph, with two temperatures., the magnitude values of the Temperature Distribution of the Stoneley wave is increases. Near the interface of the two material, the magnitude values of the temperature of the Stoneley wave are very high with two temperature and below the boundary surface, it comes to steady-state. Moreover, near the interface of the two material, the magnitude values of the temperature of the Stoneley wave show the opposite behavior without two temperature and below the boundary surface, it comes to steady-state.

Figure 10 demonstrates the Stoneley wave's displacement component w w.r.t. ξ with and without two temperatures. It is clear from the graph, with two temperatures, the displacement component w of Stoneley wave declines. Near the interface of the two material the displacement component w of Stoneley wave is very high and below boundary surface, it declines to zero. Figure 11 illustrates the stress component t_{zz} w.r.t. ξ with and without two temperatures. It is clear from the graph, with two temperatures, the stress component t_{zz} of the Stoneley wave is increased. Near the interface of the two material, the t_{zz} of Stoneley wave is very high with two temperature and below boundary surface, it comes to steady-state.

8 Conclusion

From the analysis of graphs, some concluding interpretations are:

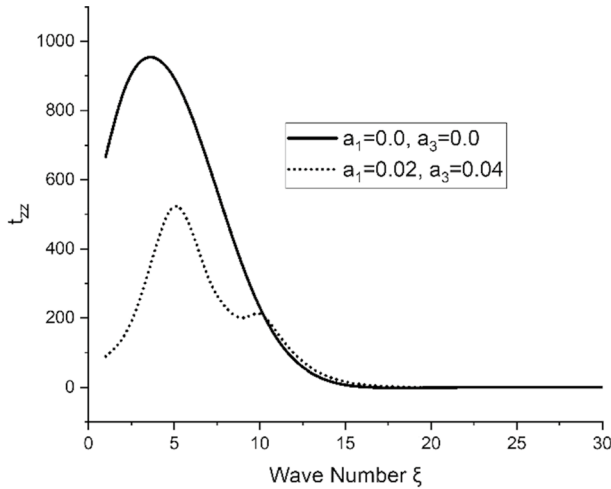


Fig. 10 Variation of Stoneley waves displacement component w w.r.t. ξ

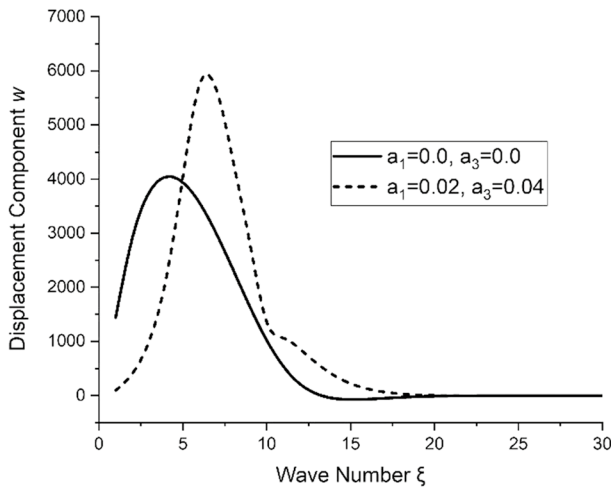


Fig. 11 Variation of Stoneley waves stress component T_{zz} w.r.t. ξ

- The Stoneley waves in a homogeneous TIT solid media with the rotation, with and without two temperatures are investigated.
- The figures clearly indicate that at the interface of the two mediums, there is a considerable influence of two temperatures and rotation on the Stoneley wave phase velocity, attenuation coefficient, displacement component, and stress component, as well as on Temperature distribution. It is also observed that the velocity of surface (Stoneley) waves not only influenced by the direction of wave propagation but as well as on the elastic properties and density of materials. The

characteristics of waves change drastically in diverse mediums and also at different depth.

- From the wave velocity equation, we find that there is a dispersion of waves due to rotation and two temperatures. The dispersive nature of the Stoneley waves is defined through the resulting Secular equation. Various special cases are also considered to approve the formulation and numerical results with the existing solutions.
- Stoneley wave's analysis provides information about the positions of fractures and permeability of the formation. These waves not only deliver better information about the internal structure of the earth but are also helpful in the assessment of valuable materials under the earth's surface. Stoneley waves are a major source of noise in vertical seismic profiles. These waves help in the study of geophysics, seismological processes, ocean acoustics, SAW devices, and non-destructive evaluation.

References

- Abd-Alla, A.M., Abo-Dahab, S.M., Khan, A.: Rotational effects on magneto-thermoelastic stoneley, love and Rayleigh waves in fibre-reinforced anisotropic general viscoelastic media of higher order. *Comput. Mater. Contin.* **53**(1), 49–72 (2017)
- Abo-Dahab, S.M.: surface waves in coupled and generalized thermoelasticity. *Adv. Mater. Corros.* **2**, 46–53 (2013)
- Abo-Dahab, S.M.: Propagation of Stoneley waves in magneto-thermoelastic materials with voids and two relaxation times. *J. Vib. Control* **21**(6), 1144–1153 (2015)
- Chandrasekharaiah, D.S.: Hyperbolic thermoelasticity: a review of recent literature. *Appl. Mech. Rev.* **51**, 705–729 (1998)
- Ezzat, M.A., El-Karamany, A.S., El-Bary, A.A.: Two-temperature theory in Green-Naghdi thermoelasticity with fractional phase-lag heat transfer. *Microsyst. Technol.* **24**(2), 951–961 (2017)
- Green, A., Naghdi, A.P.: On undamped heat waves in an elastic solid. *J. Therm. Stresses* **15**(2), 253–264 (1992). <https://doi.org/10.1080/01495739208946136>
- Hassan, M., Marin, M., Ellahi, R., Alamri, S.: Exploration of convective heat transfer and flow characteristics synthesis by Cu–Ag/water hybrid-nanofluids. *Heat Transf. Res.* **49**(18), 1837–1848 (2018)
- Kumar, R., Kumar, K., Nautiyal, R.C.: Propagation of Stoneley waves in couple stress generalized thermoelastic media. *Glob. J. Sci. Front. Res. Math. Decis. Sci.* **13**(5), 1–13 (2013)
- Kumar, R., Sharma, N., Lata, P.: Effects of thermal and diffusion phase-lags in a plate with axisymmetric heat supply. *Multidiscip Model Mater Struct (Emerald)* **12**(2), 275–290 (2016)
- Kumar, R., Sharma, N., Lata, P., Abo-Dahab, A.S.: Mathematical modelling of Stoneley wave in a transversely isotropic thermoelastic media. *Appl. Appl. Math.* **12**(1), 319–336 (2017)
- Lata, P., Kaur, I.: Transversely isotropic thick plate with two temperature and GN type-III in frequency domain. *Coupl. Syst. Mech.* **8**(1), 55–70 (2019a)
- Lata, P., Kaur, I. (2019b): Study of transversely isotropic thick circular plate due to ring load with two temperature and green Naghdi theory of type-I, II and III. In: International Conference on Sustainable Computing in Science, Technology & Management (SUSCOM-2019). Elsevier SSRN, pp. 1753–1767. Amity University Rajasthan, Jaipur
- Lata, P., Kaur, I.: Thermomechanical interactions in transversely isotropic thick circular plate with axisymmetric heat supply. *Struct. Eng. Mech.* **69**(6), 607–614 (2019c)
- Lata, P., Kaur, I.: Transversely isotropic magneto thermoelastic solid with two temperature and without energy dissipation in generalized thermoelasticity due to inclined load. *SN Appl. Sci.* **1**, 426 (2019d). <https://doi.org/10.1007/s42452-019-0438-z>

- Lata, P., Kaur, I.: Effect of rotation and inclined load on transversely isotropic magneto thermoelastic solid. *Struct. Eng. Mech.* **70**(2), 245–255 (2019e)
- Lata, P., Kumar, R., Sharma, N.: Plane waves in an anisotropic thermoelastic. *Steel Compos. Struct.* **22**(3), 567–587 (2016)
- Mahmoud, S.R.: Effect of non-homogeneity, magnetic field and gravity field on Rayleigh waves in an initially stressed elastic half-space of orthotropic material subject to rotation. *J. Comput. Theor. Nanosci.* **11**(7), 1627–1634 (2014)
- Marin, M.: An evolutionary equation in thermoelasticity of dipolar bodies. *J. Math. Phys.* **40**(3), 1391–1399 (1999)
- Marin, M., Craciun, E.: Uniqueness results for a boundary value problem in dipolar thermoelasticity to model composite materials. *Compos. B Eng.* **126**, 27–37 (2017)
- Marin, M., Craciun, E.M., Pop, N.: Considerations on mixed initial-boundary value problems for micropolar porous bodies. *Dyn. Syst. Appl.* **25**(1–2), 175–196 (2016)
- Othman, M.I., Marin, M.: Effect of thermal loading due to laser pulse on thermoelastic porous medium under G-N theory. *Results Phys.* **7**, 3863–3872 (2017). <https://doi.org/10.1016/j.rinp.2017.10.012>
- Othman, M.I., Song, Y.Q.: The effect of rotation on the reflection of magneto-thermoelastic waves under thermoelasticity without energy dissipation. *Acta Mech.* **184**, 89–204 (2006)
- Othman, M.I., Song, Y.Q.: Reflection of magneto-thermoelastic waves from a rotating elastic half-space. *Int. J. Eng. Sci.* **46**, 459–474 (2008)
- Schoenberg, M., Censor, D.: Elastic waves in Rotating media. *Q. Appl. Math.* **31**, 115–125 (1973)
- Singh, S., Tochhawng, L.: Stoneley and Rayleigh waves in thermoelastic materials with voids. *J. Vib. Control* (2019). <https://doi.org/10.1177/1077546319847850>
- Slaughter, W.S.: *The linearised theory of elasticity*. Birkhauser, Basel (2002)
- Stoneley, R.: Elastic waves at the surface of separation of two solids. *Proc. R. Soc. Lond.* **106**, 416–428 (1924)
- Tajuddin, M.: Existence of Stoneley waves at an un-bounded interface between two micropolar elastic half spaces. *J. Appl. Mech.* **62**, 255–257 (1995)
- Ting, T.C.: Surface waves in a rotating anisotropic elastic half-space. *Wave Motion* **40**, 329–346 (2004)
- Youssef, H.: Theory of two—temperature thermoelasticity without energy dissipation. *J. Therm. Stresses* **34**, 138–146 (2011)

Publisher's Note Springer Nature remains neutral with regard to jurisdictional claims in published maps and institutional affiliations.